Chapter 9. Nano-based PCMs for building energy efficiency

Dr. Kaushik Biswas
Energy and Transportation Science Division
Oak Ridge National Laboratory
Oak Ridge, TN 37831 USA
Ph: (865) 574-0917, Fax: (865) 574-9354
Email: biswask@ornl.gov

Abstract:

Thermal storage using phase change materials (PCMs) is seen as a viable method for improving the energy efficiency of buildings. PCMs have been used in building applications in various forms – PCM slurries in heat exchangers, macro- or microencapsulated PCMs in building envelopes, bulk PCM for modulating photovoltaic temperatures, etc. In the last decade a new class of PCMs, called nano-enhanced PCM (or nanoPCM), has been extensively investigated with the goal of improving the heat transfer and thermal storage properties of PCMs. NanoPCMs can primarily be categorized as nano-encapsulated PCMs and nanoparticle-PCM composites. The former are nano-sized capsules in which the PCM forms the core and is surrounded by a high-conductivity membrane or shell. The latter consist of PCM supported within nanostructures or nanoparticles dispersed in PCMs.

This article reviews the current state of nanoPCM synthesis and characterization of their heat transfer and thermal storage properties. Further, a critical review of nanoPCM applications and their potential energy benefits is performed. Nano-enhanced PCMs exhibit higher thermal conductivities than regular PCM. However, whether the higher conductivity is desirable in all applications and if the property enhancements are worth the cost and effort needed to create nanoPCMs are questions that still need to be answered.

Key words: nanoPCM, nano-encapsulated PCM, PCM-nanoparticle composite, nanoPCMs in buildings.

9.1. Introduction

Phase change materials (PCMs) have been widely investigated for thermal storage in a range of applications, including integrated collector storage solar water heater (Chaabane et al., 2014), spacecraft thermal control in extreme environments (Wu et al., 2013), phase change slurries for active cooling (Lu et al., 2012), thermal management of building integrated photovoltaic panels (Huang et al., 2006), etc. Application of PCMs to buildings to take advantage of their latent heat capacities in reducing the envelope-generated heating and cooling loads has received a lot of attention in the last two decades (Zhou et al., 2012).

PCMs in building envelopes operate by changing phase from solid to liquid while absorbing heat from the outside and thus reducing the heat flow into the building, and releasing the absorbed heat when it gets cold outside to reduce the heat loss through the building envelope. Different approaches to PCM applications in buildings have been investigated: PCM wallboards (Zhou et al., 2007; Darkwa & Su, 2012), PCM mixed in concrete and brick (Hawes & Feldman, 1992; Cabeza et al., 2007), micro-encapsulated PCM mixed with loose-fill insulation in wall cavities (Shrestha et al., 2011; Kosny et al., 2012a; Biswas & Abhari, 2014), rigid polyurethane foam incorporating fatty acid ester based PCM (Aydin & Okutan, 2013), and macro-packaged PCM in plastic pouches (Kosny et al., 2012b). Recent experimental and numerical studies have shown the potential of PCMs in reducing indoor temperature fluctuations under different weather conditions (Meng et al., 2013; Shi et al., 2014; Ascione et al., 2014), reducing energy consumption and providing peak-load shifting (Zwanzig et al., 2013), and also providing internal humidity control (Shi et al., 2014).

In a lot of PCM applications, the low thermal conductivity of traditional phase change materials is cited as a critical shortcoming. Recently, a lot of research has been focused on enhancing the thermal conductivity of PCMs by adding nanoparticles or via nano-encapsulation methods. Khodadadi and Hosseinizadeh (2007) performed one of the earliest studies pertaining to the potential of nanoparticle enhanced PCM in improving thermal storage. They predicted higher heat release rate of nanoPCMs compared to conventional PCM and contended that there is a clear potential for diverse thermal storage applications of nanoPCMs. Since then, there have been numerous studies related to synthesis of nano-enhanced PCMs and the resultant improvement in thermal properties (primarily thermal conductivity). The present article is focused on nano-enhanced PCMs and their suitability for building applications. Here, a brief review of the different kinds of PCMs is provided, followed by descriptions of synthesis methods, thermos-physical characteristics and applications of nanoPCMs. Finally, recommendations for future research are provided.

9.2. Classification of PCMs

9.2.1. Based on material

Zalba et al. (2009) and Sharma et al. (2009) reviewed phase change materials for thermal storage applications and described in detail the different PCMs based on material type. The three main PCM types defined were organic, inorganic and eutectic PCMs. Organic PCMs primarily consist of paraffins (straight chain n-alkanes), esters, fatty acids and alcohols (Sharma et al., 2009). Under inorganic PCMs, salt hydrates are primarily used. Phase transition of salt hydrates is actually a dehydration or hydration of the salt resembling melting or freezing processes thermodynamically. Salt hydrates usually melt to another salt hydrate with fewer moles of water (a) or to its anhydrous form (b), as follows:

$$(a)\ \ AB \cdot nH_2O \rightarrow AB \cdot mH_2O + (n-m)H_2O \qquad (1)$$

$$(b)\ \ AB \cdot nH_2O \rightarrow AB + nH_2O \qquad (2)$$

Metallics are another kind of inorganic PCMs but are seldom used due to weight-related issues (Sharma et al., 2009). Table 1 lists the major advantages and disadvantages of organic and inorganic PCMs. One of the drawbacks of PCMs (especially salt hydrates) is that some of them start to solidify at temperatures discernibly lower than the melting temperatures. This phenomenon is known as subcooling or supercooling, and results in inefficient utilization of PCMs.

Table 1. Advantages and disadvantages of the different PCM types

PCM Type		Advantages	Disadvantages
Organic	Paraffinic	• High latent heat of fusion • Non-corrosive • Chemical and thermal stability • Low or no subcooling	• Low thermal conductivity • Moderate flammability
	Non-paraffinic	• High latent heat of fusion • Inflammability • Low subcooling (fatty acids)	• Low thermal conductivity • Varying levels of toxicity • Instability at high temperatures
Inorganic	Salt Hydrates	• Higher volumetric latent heat • Higher thermal conductivity	• High degree of subcooling • Phase separation and segregation • Corrosiveness • Lack of thermal stability
	Metallics	• Higher volumetric latent heat • High thermal conductivity	• Weight issues

Zalba et al. (2009) and Sharma et al. (2009) provide detailed lists of various organic and inorganic PCMs, along with their melting temperatures and latent heats of fusion. Inorganic salt hydrates have melting temperatures that are relatively uniformly distributed between 8 and 130°C, and then in the 307-380°C and 700-900°C ranges. The latent heats are in the 125-

280 J/g range at low and mid-range melting temperatures and 250-450 J/g at the highest melting points. Organic PCMs have melting points in the 5-150°C range, with latent heats primarily in the 85-44 J/g range.

Finally, eutectics are minimum-melting compositions of two or more components, each of which melt and freeze congruently forming a mixture of the component crystals during crystallization. Eutectics nearly always melt and freeze without segregation since they freeze to an intimate mixture of crystals, leaving little opportunity for the components to separate. On melting both components liquefy simultaneously, again with separation unlikely (Sharma et al., 2009).

In addition to the solid-liquid transition PCM, there are solid-solid, solid-gas and liquid-gas PCM. Due to the large volume changes on the gas phase, solid-gas and liquid-gas PCMs are impractical. However, solid-solid PCMs have shown some potential. Yanshan et al. (2014) synthesized solid-solid PCMs with crosslinking structures composed of polyethylene glycols at different molecular weight as energy-storage ingredient and melamine as crosslinking functional reactant. The PCMs were melamine/formaldehyde/polyethylene glycol (MFPEG) crosslinking copolymers. The authors investigated the composition and chemical structure, thermophysical and crystallographic properties of the synthesized PCMs. The MEPEG crosslinking copolymers had high latent heats (maximum of 104-109 J/g for cooling/heating cycles) and good stability (Yanshan et al., 2014).

9.2.2. Based on packaging

Liu et al. (2015) proposed classification of encapsulated PCMs into the following categories, based on size: (i) nano-encapsulated PCM (nanoPCM) (particle size ranges between 1 and 1000 nm), (ii) micro-encapsulated PCM (microPCM) (particle size ranges between 1 and 1000 μm), and (iii) macro-encapsulated PCM (macroPCM) (particle size exceeds 1mm).

Examples of nanoPCMs, both nano-encapsulated PCM and PCMs with dispersed nanoparticles, are provided in later sections. There are several studies of application of microPCM in buildings, viz. microPCMs infused in wallboards (Darkwa & Su, 2012), concrete (Hawes & Feldman, 1992; Cabeza et al., 2007) and fibrous insulation (Shrestha et al., 2011; Kosny et al., 2012a). Biswas and Abhari (2014) experimentally and numerically investigated a macro-PCM consisting of a paraffin trapped by capillary action within the pores of mm-sized pellets of high density polyethylene (HDPE). These pellets were mixed with fibrous cellulose insulation and added to an exterior test wall. Kosny et al. (2012b) evaluated fatty acid PCMs packaged in plastic pouches in a roof application. The individual

pouches were about 5 cm x 5 cm and 2 cm high and were created by using plastic sheets of overall dimensions 0.6 m x 2.4 m.

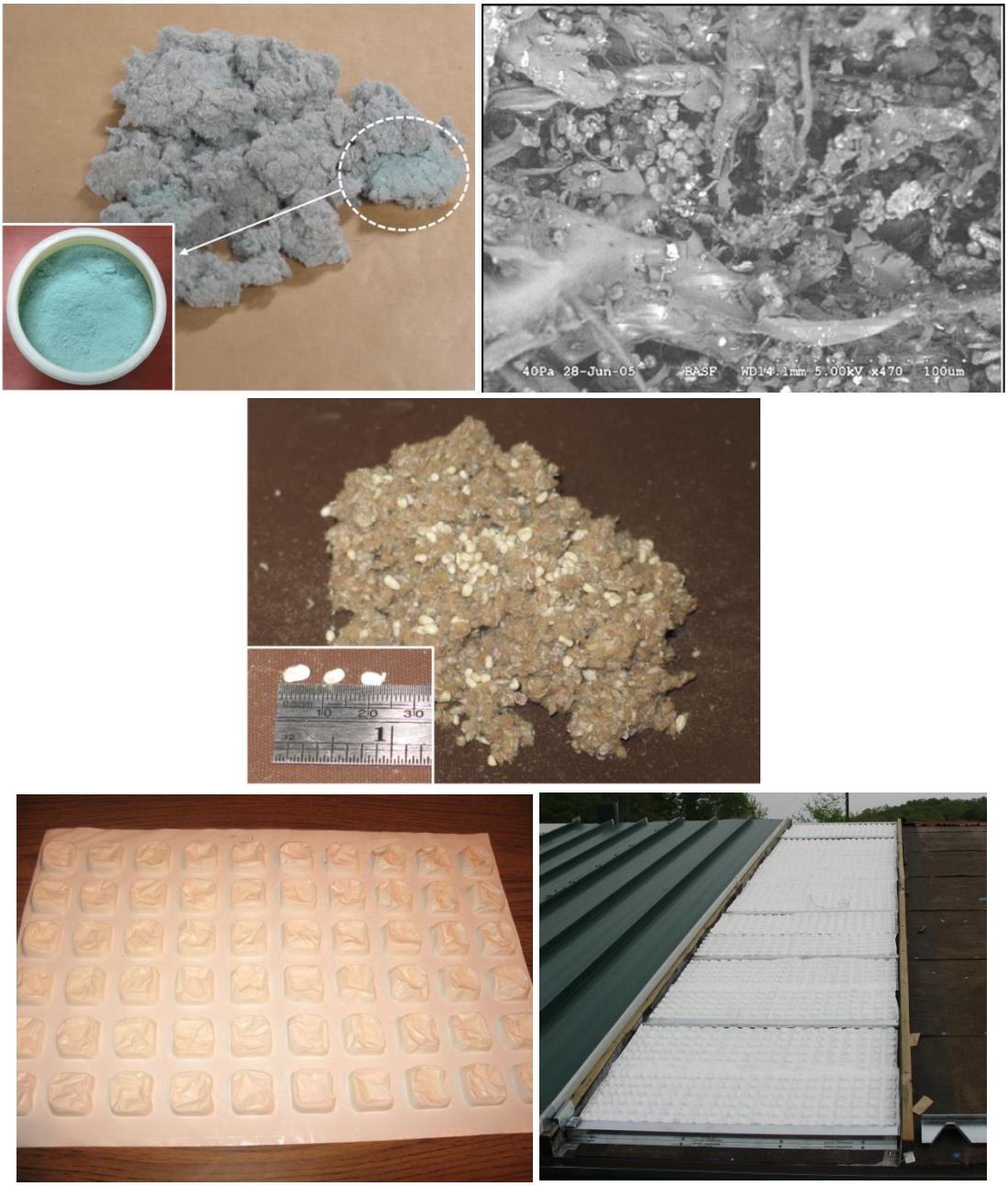

Figure 1. Photographs of selected micro- and macroPCMs. Top - PCM microcapsules mixed with fibrous insulation (Kosny et al., 2012a); Middle - millimeter-sized PCM-containing HDPE pellets mixed with fibrous insulation, studied by Biswas and Abhari (2014); Bottom – macropackaged bio-based PCM in a roof application (Kosny et al., 2012b).

9.3. Synthesis of nano PCMs

9.3.1. Nano-encapsulated PCMs

The first category of nanoPCMs can be defined as nanoencapsulated phase change materials (NEPCM), in which the PCM forms the core and is surrounded by a rigid or flexible membrane or shell. Micro- or nano encapsulated PCMs have certain inherent advantages like

less chance of the PCM reacting with the surrounding materials (more critical with inorganic PCMs) and elimination of problems related with volume change during phase transition. In a recent article, Liu et al. (2015) reviewed the literature related to preparation and characterization of nanoencapsulated PCMs and the resultant heat transfer enhancement. They identified and described in detail the following main methods of preparing nanoPCM capsules: (i) Interfacial polymerization, (ii) emulsion polymerization, (iii) miniemulsion polymerization, (iv) in situ polymerization, and (v) sol–gel method. They also discussed the suitability and relative merits of the different preparation methods for different types of PCMs and shell materials.

Sari et al. (2014) developed polystyrene(PS)/n-heptadecane micro/nano-capsules via the emulsion polymerization method with different weight ratios of polystyrene and heptadecane. Polystyrene is an inexpensive aromatic polymer and is also used as an insulation material in building applications and has reasonably good mechanical properties, which make it a good candidate for shell material on encapsulated PCMs. The particle sizes ranged from 10 nm to 40 μm for a 1:2 ratio of polystyrene and heptadecane (Sari et al., 2014). Hong et al. (2011) described the nanoencapsulation of indium nanoparticles in silica shells using the sol-gel method. They used two different silica precursors: (i) tetraethylorthosilicate (TEOS) and (ii) sodium silicate. The objective was to demonstrate reduced subcooling with sodium silicate derived silica shells of thickness 50 nm, compared to TEOS derived silica shells of thickness 100 nm. The core diameters in both cases were 200 nm. The nanoPCM with sodium silicate derived silica shells demonstrated 22-28ºC reduction in subcooling based on different cooling rates.

Park et al. (2014) described the synthesis of magnetic iron oxide (Fe_3O_4) nanoparticles (NP)-embedded PCM nanocapsules with paraffin core and polyurea shells. The synthesis was done via interfacial polycondensation between tolylene [sic] diisocyanate (TDI) and ethylene diamine (EDA) with various concentrations of the iron oxide nanoparticles, resulting in particle sizes of 400-600 nm. The purpose of creating hybrid organic-inorganic capsules incorporating adding iron oxide particles was to overcome the relatively low thermal conductivity of the polyurea shell. Micrographs of selected nano-encapsulated PCMs are shown in Figure 2.

Wang et al. (2015) used a two-step Pickering emulsification process to create NEPCM with nonadecane as the core PCM and polystyrene as the shell material. The nanoPCM capsules were observed to have fairly uniform size distribution of 734 ± 110 nm. Liu et al. (2015), in their review article, noted that the production efficiency of nanoPCM is quite low. Wang et al. (2015) claimed their method to be simple and of low-energy intensity since the

nonadecane-in-water emulsion was generated by manual shaking without need for high-energy input (i.e. sonication), so that it has promise for scale-up and mass production. The low-energy emulsification process was facilitated by the addition of zirconium phosphate platelets that reduced the surface tension in the water phase. Wang et al. (2015) also calculated the encapsulation efficiency of their NEPCM as 55.9%, using the following equation (Sánchez-Silva et al., 2010):

$$Encapsulation\ efficiency\ (\%) = \frac{\Delta H_{NEPCM}}{\Delta H_{PCM} \cdot \frac{m_{core}}{m_{shell}}} \times 100\% \qquad (3)$$

In eq. 3, ΔH is the latent heat (of the NEPCM and the regular PCM) and 'm_{core}/m_{shell}' is the core-to-shell mass ratio. The authors noted that the 55.9% encapsulation efficiency is lower than microencapsulated PCMs but comparable to other NEPCMS.

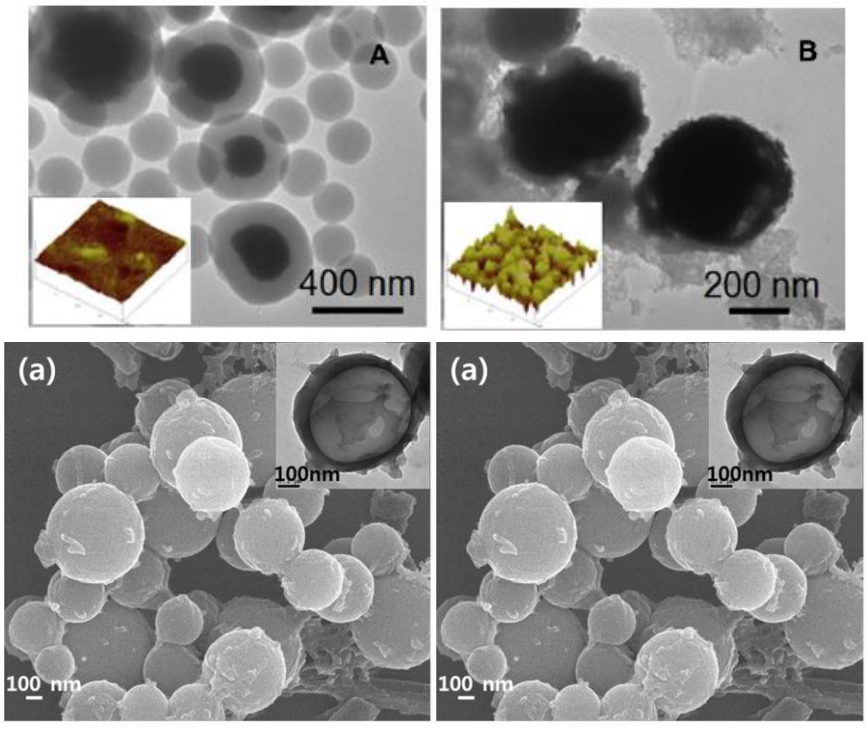

Figure 2. Micrographs of selected nano-encapsulated PCMs. Top: Indium nanoparticles encapsulated in silica derived from TEOS (A), and sodium silicate (B) (Hong et al. ,2011); Bottom: PCM nanocapsules (a) with and (b) without Fe_3O_4 nanoparticle (Park et al., 2014).

Latibari et al. (2013) synthesized nanoPCM with palmitic acid (PA) encapsulated in silica shells using the sol-gel method. The authors studied the thermal characterization and influence of different pH values on particle size. The sol solution was created by adding TEOS and ethanol (CH_3CH_2OH) to distilled water, along with ammonium hydroxide (NH_4OH) to control the pH. The nanocapsules were created by adding the sol solution into a

PA emulsion and stirring while the emulsion was kept at 70ºC. On cooling to room temperature, washing with distilled water and centrifuging, a white powder was formed and it was dried at 50ºC. Latibari et al. (2013)found that the encapsulation ratio, defined by eq. 4, increased from 83.25 to 89.55% as the pH increased from 11 to 12. The mean diameters of the nanoparticles were 183.7, 466.4 and 722.5 nm for pH values of 11, 11.5 and 12.

$$Encapsulation\ ratio\ (\%) = \frac{\Delta H_{NEPCM}}{\Delta H_{PCM}} \times 100\% \qquad (4)$$

9.3.2. Nanoparticle-PCM composites

Another category of nanoPCMs consists of PCM doped with nanoparticles or PCM absorbed within a nanoporous matrix of another higher-conductivity material. Karunamurthy et al. (2012) studied the effect on thermal conductivity by dispersing copper-oxide (CuO) nanoparticles in a paraffinic PCM. 2%-by-weight nanoparticles were dispersed in the paraffin using an ultrasonic stirrer and were found to increase the conductivity by 76%. No discussion was presented about the long-term stability of the PCM-CuO composite. Parameshwaran et al. (2013a) embedded spherical-shaped surface-functionalized crystalline silver nanoparticles (AgNP) into organic ester PCM in varying mass ratios. They found that the AgNP did not chemically react with the PCM, enabling the nanoPCM to be chemically stable. The AgNP-PCMs maintained their stability for more than three months with no observed precipitation.

Jeong and coworkers utilized a vacuum impregnation process to incorporate bio-based PCM into high-conductivity, porous structures like exfoliated graphite nanoplatelets (xGnP) (Jeong et al., 2013) and boron nitride (Jeong et al., 2014). In both studies, the chemical stability was investigated using Fourier transform infrared spectroscopy (FTIR) and it was shown that the chemical properties of the individual components did not change. The PCM molecules were retained in the pores by capillary action and surface tension and leakage of the melted PCM from the composite was prevented by these forces. Figure 3 shows scanning electron microscopy (SEM) images of bio-based PCM incorporated within nanoporous structures.

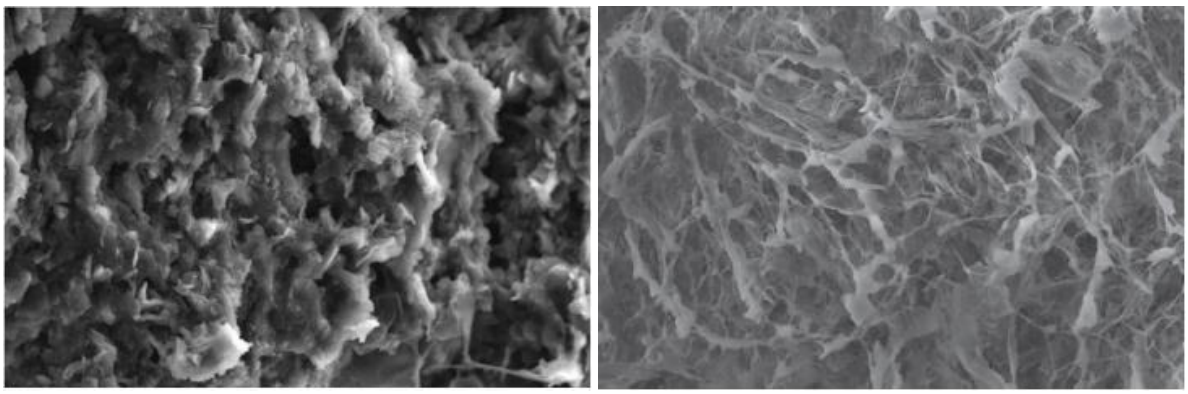

Figure 3. SEM micrographs of xGnP-bioPCM composite (left) (Jeong et al., 2013) and boron nitride-bioPCM composite (right) (Jeong et al., 2014).

Sayyar et al. (2014) and Biswas et al. (2014) reported organic PCMs (fatty acids and paraffin, respectively) supported by interconnected graphite nanosheets. Graphite nanosheets have several desirable features like high specific surface area, high thermal conductivity (1250 W/m/K), and good mechanical properties. In both cases, shape-stable blend of 92%-by-weight PCM and 8%-by-weight expanded graphite nanosheets were created and incorporated into gypsum wallboards for building envelopes. Figure 4 shows micrographs of the graphite nanosheets and nanoPCM containing n-heptadecane studied by Biswas et al. (2014).

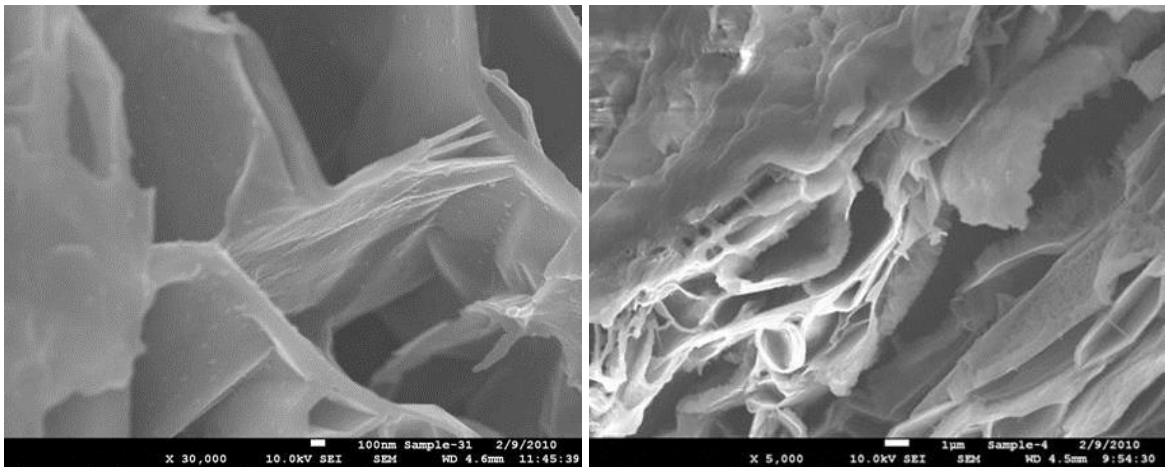

Figure 4. SEM micrographs of expanded graphite nanosheets (left) and nanoPCM (right) studied by Biswas et al. (2014).

Choi et al. (2014) manufactured PCM composites with different carbon additives, viz. multi-walled carbon nanotube (MWCNT), graphite and graphene. Poly vinyl pyrrolidone (PVP) was used as a dispersion stabilizer of carbon additives. The composites were created by adding the PVP and carbon additives to the molten PCM (stearic acid) and using an ultrasonic disruptor. It was observed that without the PVP, the MWCNTs coagulated in the liquid PCM and sediments were formed in seven days, but with the PVP the dispersion was

maintained for two days. With graphene and graphite, sedimentation without PVP occurred in five and two days, but with PVP the dispersions were maintained for eight and three days, respectively.

Alshaer et al. (2013) developed paraffin wax-based nanocomposites with MWCNT loadings of 0, 0.25, 0.50 and 1% by weight. Both single- and multi-wall carbon nanotubes were candidates, but the authors chose MWCNTs since they can be produced on an industrial scale. The MWCNTs had lengths ranging from 0.1 to 10 mm, outer mean diameter in the range of 10-15 nm, and number of walls between 10 and 15. The MWCNT containing granules were immersed in the molten paraffin and dispersed using a high-speed rotor, followed by sonication to homogenize the dispersion. Finally, the samples were agitated under vacuum to reduce the trapped air bubbles. Figure 5 shows micrographs of MWCNTs and MWCNTs dispersed in a paraffin matrix.

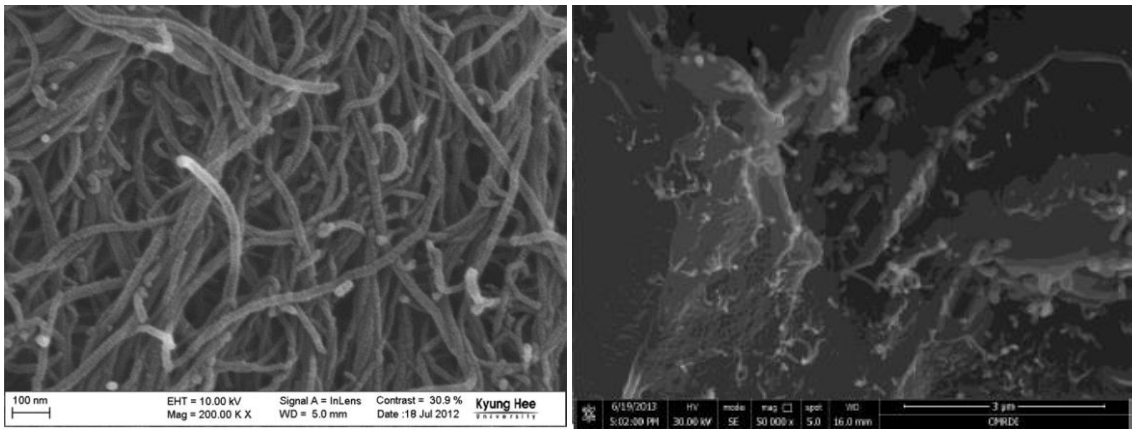

Figure 5. SEM micrographs MWCNTs (left) (Choi et al., 2014) and 1%-by-weight MWCNTs dispersed in a paraffin matrix (Alshaer et al., 2014).

9.4. Characterization of nano PCMs

9.4.1. Thermo-physical properties

Liu et al. (2015) reviewed the characteristics and heat transfer enhancement of NEPCMs synthesized via different polymerization and sol-gel methods. In another review article, Kibria et al. (2015) discussed the impact of nanoparticles dispersed in PCMs on the following: (i) thermal conductivity, (ii) latent heat capacity, (iii) subcooling, and (iv) viscosity. Parameshwaran and Kalaiselvam (2015) wrote a recent survey article on nanomaterial-embedded PCMs, in which they discussed the thermal energy storage properties including conductivity, phase change temperature and latent heat, nucleation and energetic aspects of nanoPCMs.

Park et al. (2014) studied magnetic iron oxide (Fe_3O_4) nanoparticles (NP)-embedded PCM nanocapsules with paraffin core and polyurea shells and found that the thermal conductivity

increased with higher concentration of Fe_3O_4) nanoparticles, from 0.23 W/m/K to about 0.33 W/m/K. Latibari et al. (2013) reported an increase in thermal conductivity of palmitic acid by nanoencapsulation in silica shells compared to the base PCM; from 0.21-0.26 W/m/K to 0.47-0.77 W/m/K based on the nanocapsule sizes. Melting and freezing temperature changes were within 1.3 and 1.9ºC and the maximum degradation in latent heat was 16.7% during melting and 18.2% during freezing. Karunamurthy et al. (2012) found a 75% increase in thermal conductivity by addition of 2%-by-weight CuO nanoparticles to a paraffin. Jeong et al. (2013) prepared stable bio-based PCMs with exfoliated graphite nanoplatelets (xGnP), via vacuum impregnation method with the goal of improving the thermal conductivity and fire retardant properties. At 75% incorporation rate the latent heats reduced to 110.6 and 115 J/g for melting and freezing compared to 149.2 and 133.5 J/g of the base PCM. Both melting and freezing points were lowered by 1.9 and 1.2°C, with a 375% increase in thermal conductivity. Biswas et al. (2014) measured the thermal conductivity of gypsum wall board containing 20%-by-weight nanoPCM to be 0.41-0.43 W/m/K compared to 0.15 W/m/K of regular gypsum board. Yavari et al. (2011) created a nanoPCM with graphene and 1-octadecanol, and found an increase of 140% in thermal conductivity without significant loss of latent heat. Zeng and co-workers (Zeng et al., 2009; Zeng et al., 2010) created nanoPCM with dispersed carbon nanotubes and silver (Ag) nanowires and found greater thermal conductivity enhancement with Ag nanowires.

Meng et al. (2012) studied various fatty acids and their mixtures with different weight percentages of carbon nanotubes (CNTs) (0-50%) and studied the effect on melting and crystallization temperatures and latent heats. For 10-20% CNTs the latent heats dropped by 13-27%, and the drop was higher with higher fraction of CNTs. On the other hand, the melting and freezing temperatures dropped irregularly with increasing CNT fraction. Ho and Gao (2009) looked at 5 and 10%-by-weight of nano alumina (Al_2O_3)-in-octadecane emulsions and observed minimal changes in melting and freezing points while the latent heat degraded by 7 and 13%. Alshaer et al. (2013) made an interesting observation of significant rise in latent heat with addition of MWCNTs compared to the base paraffin (up to 8.5%).

Hong et al. (2011) found that nanoPCM with sodium silicate derived silica shells demonstrated 22-28ºC reduction in subcooling based on different cooling rates. Zhang et al. (2013) studied the role of carbon nanotubes as nucleating agents in hexadecane. The freezing temperature of the PCM slurry changed based on the concentration of the CNTs. The degree of subcooling varied from 6.5°C at 0% CNTs to a minimum of 3.5°C at 0.2% of CNTs by weight, with irregularly varying reductions at other CNT concentrations. Kibria et al. (2015) noted that ‘to act as a nucleating agent’ the dispersed particle should have a similar structure

to the base fluid. He et al. (2012) experimented with titanium oxide (TiO_2) particles dispersed in barium chloride hydrate solution ($BaCl_2$-H_2O). The energy barrier the needs to be overcome for crystal growth is a function of the specific surface free energy between the crystal nuclei and the nanoparticles; lower the surface free energy, lower the energy barrier. In the study by He et al. (2012), the TiO_2 particles were sized about 20 nm, close to the size of the crystal nuclei the $BaCl_2$–H_2O solution resulting in small surface free energy, and the degree of subcooling was near zero at the volume fraction of TiO_2 of 1.13%. A similar observation of near-zero subcooling was made by Hu et al. (2011) by mixing 5%-by-weight of aluminium nitride (AlN) nanoparticles in sodium acetate trihydrate (SAT) ($CH_3COONa \cdot 3H_2O$). Parameshwaran et al. (2013b) investigated the nucleation and freezing in a hybrid nanocomposite-dibasic ester PCM. Figure 6 shows the nucleation sites, solid-liquid interface formation and the progress of the freezing process observed by Parameshwaran et al. (2013b).

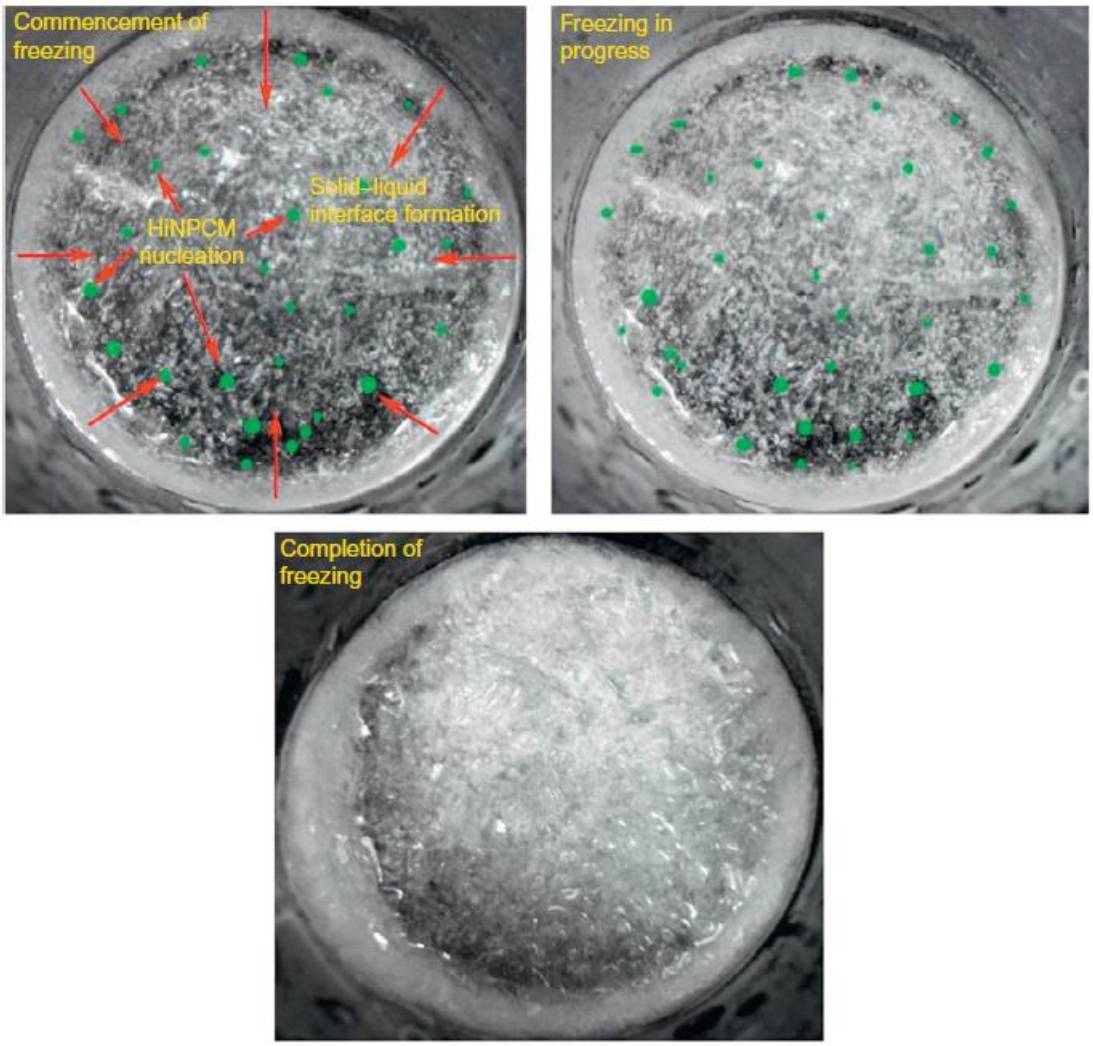

Figure 6. Pictorial representation of the freezing process in a hybrid nanoPCM (Parameshwaran et al., 2013).

Sayyar et al. (2014) and Biswas et al. (2014) describe PCM supported within expanded graphite nanosheets. The meso- and macro-pores between the nanosheets provided high liquid sorption capacity and the molten PCM was immobilized within the pores by capillary action and surface tension. This provides shape-stability even when the nanoPCM is maintained beyond the melting temperature, as seen in Figure 7. Jeong and coworkers (Jeong et al., 2013; Jeong et al., 2014) reported similar form-stable PCMs where bio-based PCM was absorbed into porous structures of boron nitride and xGnP.

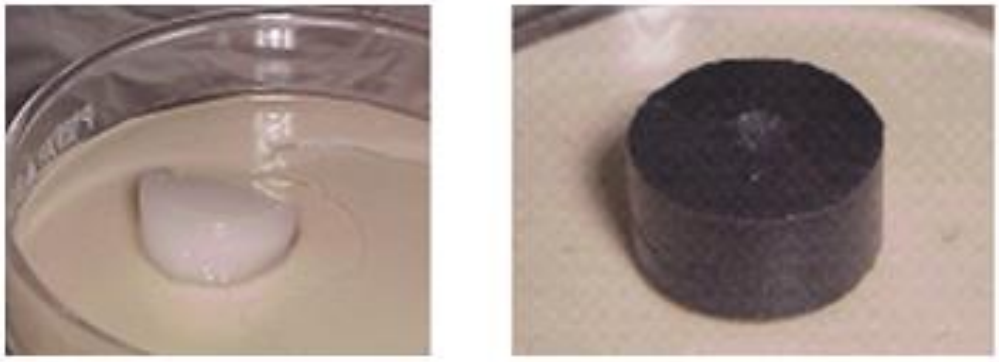

Figure 7. Shape stability of nanoPCM studied by Biswas et al. (2014); both heptadecane (left) and nanoPCM (right) were held at 10°C above the melting temperature.

9.4.2. Test methods for thermal characterization

Characterization of the thermal storage properties of PCMs (including nanoPCMs) is usually done via differential scanning calorimetry (DSC), a standard method for thermal analysis (Gmelin & Sarge, 2000). However, several studies have shown that the measurement conditions, specifically the heating and cooling rates, may result in artifacts in the measured data. Castellon et al. (2008) (and other articles by the same group of researchers) have shown that in the continuous cooling mode and at high cooling rates, the DSC traces show significant subcooling. The degree of subcooling is sensitive to the cooling rate and is smaller at slower cooling rates. To overcome the 'artificial' subcooling issue, a 'step' DSC method has been proposed. Castellon et al. (2008) presented data based on both the continuous heating/cooling and the 'step' methods. In the 'step' method, rather than constant heating and cooling, small heating/cooling ramps are followed by periods in which the temperature is kept constant to allow the PCM sample to equilibrate. Unlike the constant heating and cooling mode, where heat absorption/release peaks are only seen during melting/freeing, in the 'step' mode heat flux signal has a series of small peaks corresponding to the temperature steps. The enthalpy as a function of temperature ($h(T)$) is determined by integration of the heat flux peaks.

Another potential issue with DSC is that measurements are taken on small, mg-sized samples of the PCMs. For the DSC data to be representative of the real PCMs used in building applications there is the inherent assumption of the homogeneity of larger-scale PCM samples, which may not be accurate. Further, heating/cooling rates of 1, 5, 10 and even 20°C per minute are used in DSC measurements. In building envelope applications, the PCMs could be subjected to much lower temperature change rates (~1°C or less per hour). Thus, the DSC data could be severely misrepresenting the PCM behavior. To overcome these issues, a recent ASTM International standard, C1784 (2013), has been developed. It is a test method analogous to the 'step' DSC method and is performed using a heat flow meter apparatus (HFMA). This test method is based on a modification of the HFMA technology (hardware

and software) developed for steady-state thermal transmission property measurements of planar, homogeneous materials (ASTM C518, 2010).

The HFMA consists of two independently temperature-controlled plates that sandwich the test specimen. The plates are also equipped with surface heat flux transducers to measure the heat absorbed or released by them. ASTM C1784 is a dynamic test method in which a series of measurements are made to determine the enthalpy storage of a test specimen over a temperature range. First, both HFMA plates are held at the same constant temperature until steady state is achieved. Steady state is defined by the reduction in the amount of energy entering the specimen from both plates to a very small and nearly constant value. Next, both plate temperatures are changed by identical amounts and held at the new temperature until steady state is again achieved. The enthalpy absorbed or released by the specimen from the time of the temperature change until steady state is again achieved is recorded. Using a series of temperature step changes, the cumulative enthalpy stored or released over a certain temperature range is determined. The storage capacity of a PCM is well defined via four parameters: specific heats of both solid and liquid phases (via slope of the enthalpy functions), phase change temperature range and phase change enthalpy (latent heat).

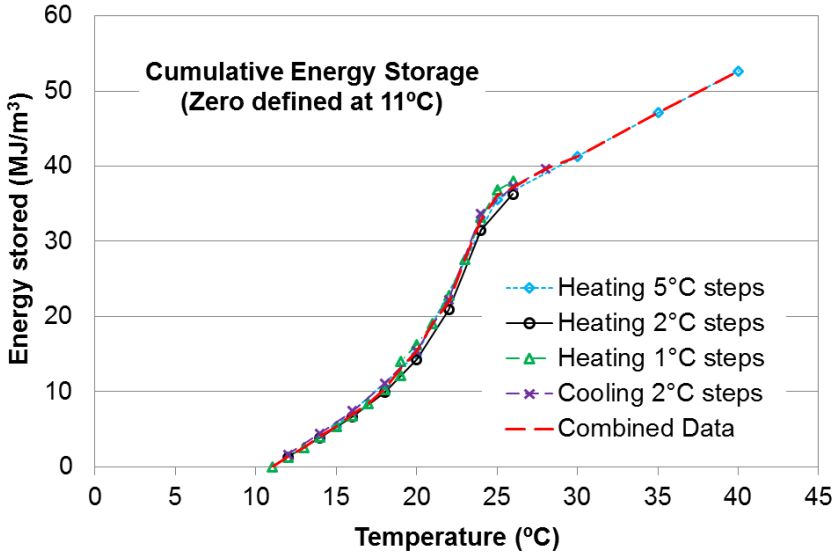

Figure 8. Measured volumetric energy storage of a sample PCM from heating and cooling tests using ASTM C1784 (2013)[1].

Figure 8 shows data from heating and cooling tests of an organic PCM. The heating tests were performed with different temperature steps. For this test method, it is recommended that

[1] Reprinted, with permission, from ASTM C1784–14 Standard Test Method for Using a Heat Flow Meter Apparatus for Measuring Thermal Storage Properties of Phase Change Materials and Products, copyright ASTM International, 100 Barr Harbor Drive, West Conshohocken, PA 19428. A copy of the complete standard may be obtained from ASTM, www.astm.org

the measurements should start at temperatures well below the melting initiation point of the PCM and continue till well after the melting end point is reached (or vice-versa for cooling tests). This test is applicable to macro-scale PCMs or products and composites containing PCMs. The rationale for developing this test method was that the mg-sized samples tested via DSC may not be representative of the relationship between temperature and enthalpy storage of full-scale PCM products.

The RAL Quality PCM Association[2] was founded in 2004 by several international PCM-related enterprises with the goal of developing proper quality assurance procedures and guaranteeing the quality of thermal storage materials. The fundamental quality criteria are the stored heat as a function of temperature, the number of possible repetitions without any adverse effects and the thermal conductivity of the storage materials which is important for the charge and discharge time. The Quality PCM Association's publication, RAL-GZ (2009), is another standard that provides guidelines for measurement and reporting of data related to thermal storage characteristics of PCMs.

Several researchers have evaluated the stability of thermal properties, chemical structure and volume change of PCMs by subjecting them to accelerated aging via rapid melting and freezing cycles. Latibari et al. (2013) investigated properties of nanoencapsulated palmitic acid-in-silica shell PCM after 2500 thermal cycles. The latent heat of the tested PCM changed from 180.9 kJ/kg to 177.3 kJ/kg during melting and from 181.2 kJ/kg to 178.6 kJ/kg during freezing. Sari et al. (2003) evaluated the reliability of various fatty acid PCMs after 120, 560, 850 and 1200 thermal cycles. It was observed that the melting temperature tended to decrease after 560 and then 1200 cycles. The latent heat also decreased with increasing number of cycles but in an irregular manner. Sharma et al. (1999) subjected a fatty acid PCM to limited numbers of thermal cycles (20-300) and found no degradation in melting temperature and latent heat of fusion. Karaipekli et al. (2009) and Fauzi et al. (2014) performed accelerated aging tests on eutectic mixtures of fatty acid. Karaipekli et al. (2009) did up to 5000 thermal cycles and observed irregular changes in melting temperature and latent heat; the authors however, contended that the changes were within acceptable limits for thermal storage applications. Fauzi et al. (2014) did 200, 500, 1000 and 1500 thermal cycles of two mixtures of fatty acids - myristic acid/palmitic acid (MA/PA) (70/30, wt.%) and 5%-by-weight sodium stearate (SS) added to 70/30 (wt.%) MA/PA mixture. They also reported irregular but acceptable changes in the melting temperatures. The latent heat of MA/PA/SS decreased by 10.1% after 1500 cycles, while that of MA/PA increased by up to 6%. Some

[2] http://www.pcm-ral.de/en/quality-association.html

structural and volume changes were also noticed by the authors. The 1500 cycles represented 4 years of utilization, presumably by assuming one thermal cycle per day.

Similar aging tests are needed for nano-enhanced PCMs. Further, it needs to be determined if the rate of heating and cooling used in the aging tests create some artifacts in the measured data, similar to that observed in the DSC traces with respect to subcooling of PCMs (Castellon et al., 2008). Also, whether or not the changes or degradation in thermal properties are acceptable needs to be determined by coupling such aging tests with energy-savings evaluation studies. For example, if the latent heat degrades, what impact does it have on the energy-savings potential of PCM over the life of the application and how will the cost-to-savings ratio change?

9.5. Building Applications

Several researchers have presented experimental and numerical studies of melting/freezing of nanoPCMs within containers and heat exchangers. Hosseinizadeh et al. (2012) numerically investigated the unconstrained melting of a nanoPCM consisting of RT27 and copper particles in a spherical container. RT27 is a commercially available PCM[3] with a melting temperature of 28/30°C and latent heat of 179 kJ/kg. Initially the PCM was assumed to be at 6°C below its melting points and then was heated by maintaining the container wall temperatures at 5, 10 and 15°C above its melting temperature. The higher conductivity and lower latent heat resulted in higher melting rate of the nanoPCM (Hosseinizadeh et al., 2012). Dhaidan et al. (2013) experimentally and numerically studied the melting of nanoPCM under constant heat flux boundary conditions. Addition of nanoparticles enhanced the thermal conductivity and melting rate and expedited the melting time of the PCM. The rate of increase in the melting process was higher at lower values nanoparticle loading, which has additional benefits of higher energy storage capacity and lower cost compared to higher loadings.

Abolghasemi et al. (2012) performed a second law analysis of a thermal storage unit consisting of two concentric cylinders. The outer cylinder was filled with the PCM (calcium chloride hydrate, $CaCl_2.6H_2O$) and the working fluid (water) flowed through the inner cylinder. Addition of nanoparticles to the PCM reduced the melting period, entropy generation and stored energy. However, the reductions were of different magnitudes; for example, in one case an 11% reduction in stored energy was accompanied by 44% reductions in both melting period and entropy generation leading to more efficient heat transfer.

[3] Rubitherm GmbH, http://www.rubitherm.eu/

Parameshwaran and Kalaiselvam (2014) did a study aiming to improve the thermal performance and energy efficiency of chilled water based variable air volume (VAV) air conditioning (A/C) system integrated with the silver nanoparticles embedded latent thermal energy storage system (NTES). The NTES-VAV A/C system was investigated with demand control ventilation (DCV) and combined DCV-economizer cycle ventilation (ECV). For comparison, a conventional constant air volume (CAV) and a VAV A/C systems were also considered. These A/C systems were designed for operation in a hot and arid climate zone. The proposed NTES-VAV A/C systems achieved 36–58% and 24–51% of on-peak and per day average energy savings, respectively, compared to conventional CAV A/C system. For the same operating conditions, the proposed A/C system while compared with a basically similar VAV A/C system yielded 7.5% to 18.6% of energy savings. However, the impacts of the nanoPCM versus DCV/ECV were not isolated.

Groulx (2015) asked an interesting and relevant question – Are nanoPCMs worth it? In his numerical study, Groulx looked at the melting and freezing of a nanoPCM and regular PCM in a container. Metallic fins were assumed within the container with the base PCM. The base PCM with the fins outperformed the nanoPCM in both storing thermal energy and achieving higher heat transfer rates. The study did not consider any subcooling in the base PCM nor the reduction in subcooling in the nanoPCM, and their impact on PCM melting and freezing.

Sayyar et al. (2014) evaluated the energy impacts of a gypsum wallboard containing fatty acid PCM incorporated with graphite nanosheets. Testing of the nanoPCM wallboard was performed in one of two side-by-side test cells of 0.28 m sides, with the other test cell containing regular gypsum board. The test cells were placed in a climatic chamber in which the temperature was varied to simulate outside temperature time-histories with slow and rapid temperature changes. The resulting temperatures within the test cells were monitored. The experimental work was coupled with simulations to estimate the energy savings. Models of a room with 1 m x 1 m walls with and without the nanoPCM were created. Measured exterior and interior test cell wall temperatures were used as inputs to the numerical models to calculate the wall heat fluxes. The models were also used to estimate the energy demands to maintain the two cells at comfortable conditions. For the assumed conditions, a reduction in energy demand of 79% was estimated when the walls contained the nanoPCM.

Biswas et al. (2014) also studied the performance of nanoPCM-gypsum boards via experimental and numerical means. This is one of the few studies of combining experimental evaluation of nanoPCM in a real building with validated numerical simulations for annual

energy benefits. It should be noted however, neither study compared the performance of the nanoPCM to regular PCM-enhanced gypsum boards.

In the study by Biswas et al. (2014), a gypsum board containing 20%-by-weight dispersed nanoPCM was installed in an exterior wood framed wall in a conditioned building in a warm climate; the same wall contained another section covered with regular gypsum board served as the baseline. The test wall was instrumented with temperature and heat flux sensors, and was monitored over nine months covering the summer, autumn and winter seasons. The measured data were used to validate two-dimensional numerical models that were created to match the actual test wall. Once validated, the numerical models were used to estimate the energy-savings from the nanoPCM wallboard on an annual basis. An enthalpy function, shown in Figure 9, was calculated using DSC heat flow data and used as input to the model for the PCM thermal storage properties (melt fraction, specific heat and latent heat).

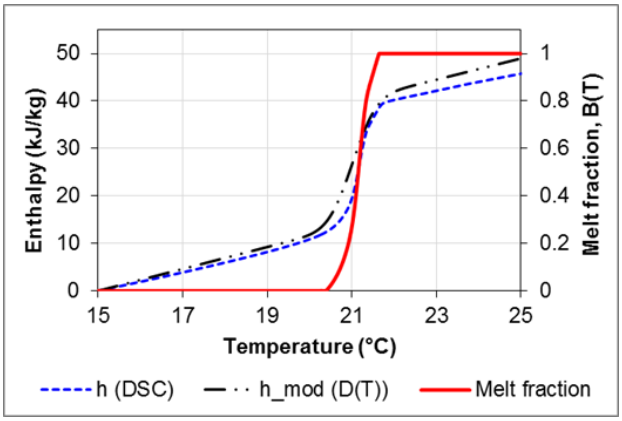

Figure 9. NanoPCM wallboard enthalpies (h) and melt fraction as functions of temperature (Biswas et al., 2014).

For the annual simulations, appropriate exterior and interior boundary conditions were required. For the exterior side, data from typical meteorological year (TMY3) weather files were used; this included solar radiation, convection heat transfer based on exterior temperatures and wind conditions, and radiation exchange with the surroundings. On the interior side, a constant surface heat transfer coefficient was assumed to calculate the heat transfer between the wall surface and the interior conditioned space (room). Heat gains and losses at the interior wall surface were calculated and used for comparing the performance of the nanoPCM and gypsum wallboards. Finally, the time-delay in heat transfer caused by the melting/freezing of the PCM has the potential to further reduce cooling air conditioning electricity consumption. This is because a lot of air conditioning equipment are placed outdoor and operate at higher efficiency when the outside temperatures are lower. This effect was investigated by converting the wall heat gains to electricity consumption, using assumed temperature-dependent energy efficiency ratios (EER) for heat pumps.

The thermal conductivities of the nanoPCM containing wall board and regular gypsum board were measured using ASTM C518 (2010). The nanoPCM wall board was tested at temperatures fully above and below the melting range of the PCM and are listed in Table 2. The effective conductivity (k) was calculated as a function of the solid (s) and liquid (l) state conductivities and the melt fraction (B), as follows:

$$k(T) = k_s + (k_l - k_s)B(T) \quad (5)$$

Table 2. Measured thermal conductivities of the gypsum and nanoPCM wallboard (Biswas et al., 2014)

	Density (kg/m^3)	Thermal conductivity (W/m/K)	Specific heat (kJ/kg/K)	Latent heat (kJ/kg)
Gypsum	549.5	0.153	1.089	--
NanoPCM wallboard	658.5	0.410 (s)	2.312 (s)	26.2
		0.427 (l)	2.236 (l)	

An interesting finding of the study was that the energy savings due to the nanoPCM were sensitive to the interior heating-cooling set points. Figure 10 shows the heat flows at the interior surface of a south oriented wall or different set points (20-23.3, 20-22 and 19-21°C). Heat flows through the modeled wall with nanoPCM wallboard ('NP-Gyp') and regular gypsum board ('Gypsum') are shown. Figure 10 also shows the calculated monthly cooling electricity consumption for the different set points.

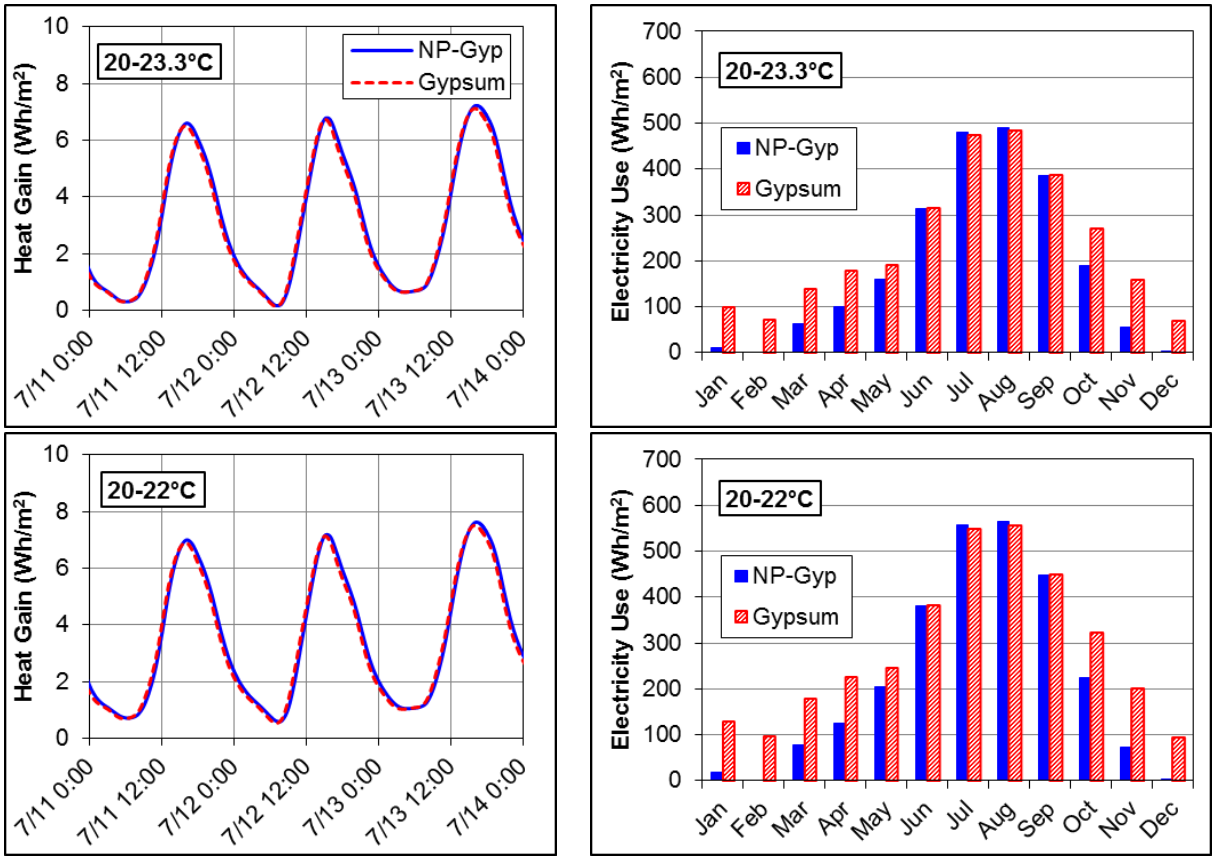

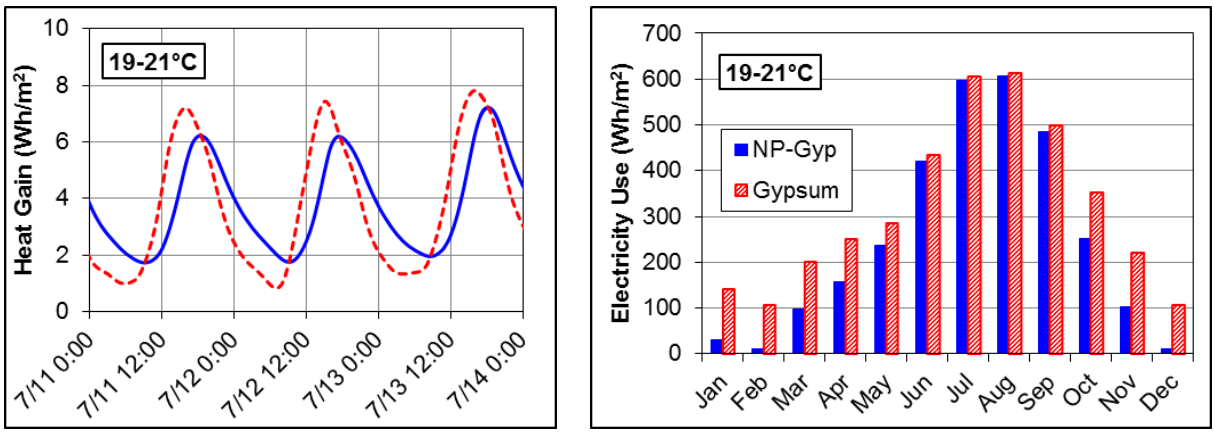

Figure 10. Left – calculated heat gains through the nanoPCM (NP-Gyp) and regular gypsum wall boards on a south oriented wall; Right – calculated monthly cooling electricity use (Biswas et al., 2014).

Table 3 shows the percentage annual reductions in heat gain and cooling electricity use for the different set points. During peak summer, peak daytime heat flow reductions are seen at the 19°C cooling set point (Figure 10), which is in the middle of the phase change temperature range of the nanoPCM. However, the greatest reductions in annual heat gain and electricity use were observed at the 22°C cooling set point, which is slightly higher than the upper temperature limit of the phase change.

Table 3. Calculated energy savings with the nanoPCM wallboard compared to gypsum wallboard (Biswas et al., 2014)

Set Points	Heat gain (Wh/m^2)		% Difference	Cooling Electricity Use (Wh/m^2)		% Difference
	Gypsum	NP-Gyp		Gypsum	NP-Gyp	
19-21°C (66-70°F)	15379.2	12191.2	-20.73	3815.8	3010.1	-21.12
20-22°C (68-72°F)	13768.6	10375.2	-24.65	3427.3	2676.6	-21.90
20-23.3°C (68-74°F)	11292.2	8639.5	-23.49	2836.5	2246.9	-20.78

The analysis by Biswas et al. (2014) can be extended to evaluate the impact of the enhanced thermal conductivity of the nanoPCM. The thermal conductivity of nanoPCM gypsum was 0.41-0.43 W/m/K compared to 0.15 W/m/K of regular gypsum board. When the nanoPCM is fully molten/frozen, the thermal conductivity of the nanoPCM wallboard is higher than that of regular gypsum board. So, the higher conductivity may become a liability unless the PCM is always in the transition state. This could explain the higher calculated cooling electricity use with the nanoPCM wallboard shown in Figure 10 during the two peak summer months (July and August) for the 23.3 and 22°C cooling set points. To further investigate this effect, an additional simulation was run by setting the thermal conductivity of the nanoPCM wallboard to that of regular gypsum board (0.15 W/m/K).

Figure 11 compares the monthly heat gains through a south oriented wall for the different wallboards. It is clear that with the nanoPCM wallboard with the reduced conductivity, the total monthly heat gains were minimum during the peak summer months. On annual basis, the nanoPCM wallboard with higher conductivity reduced the heat gain by 23.5% compared to the regular gypsum board, while the nanoPCM wallboard with lower conductivity reduced the heat gain by 24.6%. Thus, the higher conductivity of the nanoPCM wasn't beneficial for this particular application. Similar energy-related investigations are needed for other potential applications to justify the development of nanoPCMs with enhanced thermal conductivity.

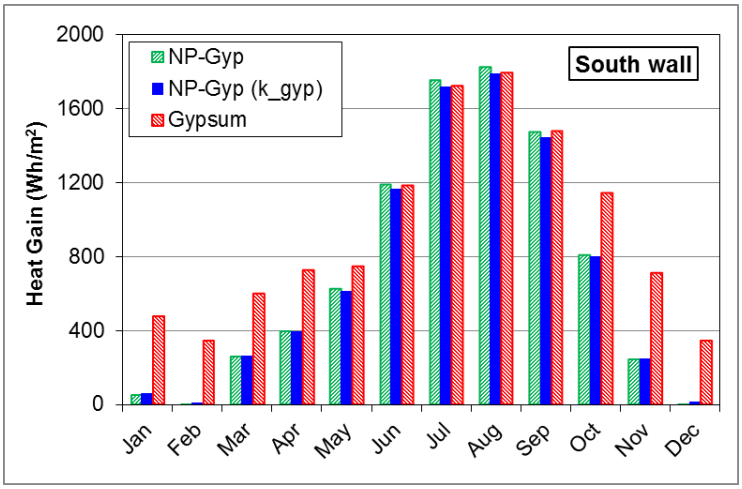

Figure 11. Comparison of the calculated heat gains due to nanoPCM wallboard, nanoPCM wallboard with lower conductivity ('k_gyp') and regular gypsum board.

While experiments and modelling of the heat transfer processes within PCM are important in characterizing PCMs, whole building or building systems-level simulations are necessary for determining the techno-economic feasibility of PCMs. Al-Saadi and Zhai (2013) reviewed the modelling of PCMs embedded in building enclosures. The authors discussed the different numerical formulations (enthalpy method, heat capacity method, temperature transforming method and heat source method), PCM models (simplified, intermediate and sophisticated) and integration of PCM models in major building simulation tools (EnergyPlus[4], TRNSYS[5], ESP-r[6], etc.), as well as their advantages and limitations. The intermediate models are most commonly used; these models are trade-offs between the rough approximations of the physical processes occurring in PCMs of simplified models and the sophisticated models created using well validated numerical packages with optimized numerical methods. Al-Saadi and Zhai (2013) also reviewed several whole building

[4] http://apps1.eere.energy.gov/buildings/energyplus/

[5] http://sel.me.wisc.edu/trnsys/

[6] http://www.esru.strath.ac.uk/Programs/ESP-r.htm

simulation models that perform computations on an hourly or sub-hourly basis while considering the dynamic interactions between all thermal-based elements related to energy consumption, including the building envelope, heating and cooling systems, lighting, etc. The authors noted that most whole building simulation programs incorporate PCM models based on the heat capacity method, which necessitates use of time steps of the order of minutes (rather than hourly) and makes the simulation programs computationally inefficient. Further, the most commonly used models do not have the capability to model the hysteresis or subcooling that is inherent in most PCMs. Finally, Al-Saadi and Zhai (2013) concluded by emphasizing the need for more research to investigate the performance of different PCM models under different climatic and operating conditions.

9.6. PCM Manufacturers

The Quality PCM Association lists several PCM manufacturers from different countries as its members[7]. These members produce a wide range of PCM products, including organic and inorganic materials, as macro- and microencapsulated PCMs, and PCMs for low, ambient and high temperature applications. Several of these members, like BASF[8] and Rubitherm[9], have a global presence with worldwide partners and suppliers. Based on the articles reviewed in this chapter, Table 4 and Table 5 provide brief lists of manufacturers and suppliers of PCMs and chemicals, precursors, etc., used to produce nanoshells for NEPCM and nanoparticles, nanosheets, etc., for the nanoPCM composites.

Table 4. Manufacturers and suppliers of selected PCMs

Paraffin (55.3°C, 151.9 J/g) (Park et al., 2014)	Sigma-Aldrich, Milwaukee, WI, USA (www.sigmaaldrich.com/)
Palmitic acid (Latibari et al., 2013)	Fisher Scientific Inc. (www.fishersci.com/us/en/home.html)
Bio-based PCM (Jeong et al., 2013; Jeong et al., 2014)	Korea C&S Corporation (www.koreacns.com/)
Capric acid and palmitic acid (Sayyar et al., 2014)	Sigma Aldrich (www.sigmaaldrich.com/)
Stearic acid (Choi et al., 2014)	Dae-Jung Chemical & Metal (daejungchem.lookchem.com/)
Paraffin wax RT65 ($C_{30}H_{62}$) (Alshaer et al., 2013)	Rubitherm Technologies Gmbh (www.rubitherm.eu/en/)

[7] http://www.pcm-ral.de/en/members.html

[8] https://www.basf.com/en.html?

[9] http://www.rubitherm.eu/en//index.html

Sodium acetate trihydrate (SAT) (Hu et al., 2011)	Sinopharm Chemical Reagent Co., Ltd., Shanghai, China (shreagent.lookchem.com/)
Myristic acid and palmitic acid (Fauzi et al., 2014)	Acros Organic (www.acros.com/)
N-octadecane (Dhaidan et al., 2013)	Sigma-Aldrich, St. Louis, MO, USA (www.sigmaaldrich.com/)

Table 5. Manufacturers and suppliers of materials for preparation of nanoparticles, nanoshells, etc.

Tolylene diisocyanate (TDI) and ethylene diamine (EDA) (for polyurea shells); Ferric chloride ($FeCl_3 \cdot 6H_2O$), ferrous chloride ($FeCl_2 \cdot 4H_2O$) (for Fe_3O_4 nanoparticles) (Park et al., 2014)	Sigma-Aldrich, Milwaukee, WI, USA (www.sigmaaldrich.com/)
Tetraethoxysilane ($SiC_8H_{20}O_4$) (TEOS) (98%) (precursor for silica shell) (Latibari et al., 2013)	Fisher Scientific Inc. (www.fishersci.com/us/en/home.html)
Silver nitrate (AgNP precursor) (Parameshwaran et al., 2013a)	Ranbaxy (part of Sun Pharma, www.sunpharma.com/)
Sulfuric acid-intercalated expandable graphite (to produce xGnP) (Jeong et al., 2013)	Asbury Graphite Mills, NJ, USA (asbury.com/)
Boron Nitride (Jeong et al., 2014)	Momentive Performance Materials Inc. (www.momentive.com/)
Exfoliated graphite nanoplatelets (xGnP) (Sayyar et al., 2014)	XG Sciences (xgsciences.com/)
Interconnected graphite nanosheets (Sayyar et al., 2014)	Drzal group, Michigan State University (www.msu.edu/)
MWCNT (Choi et al., 2014)	CNT Co., Ltd.
Graphene nanopowder (Choi et al., 2014)	Enanotec (www.enanotec.co.kr/)
Graphistrength® (with 20%-by-weight MWCNT) (Alshaer et al., 2013)	Arkema, France (www.arkema.com/en/)
Aluminium nitride (AlN) (Hu et al., 2011)	Kaier Nanometer Energy & Technology Co., Ltd., Hefei, China (www.nano-powders.com/)
Sodium stearate (Fauzi et al., 2014)	Sigma Aldrich (www.sigmaaldrich.com/)
CuO nanoparticles (Dhaidan et al., 2013)	Chemistry Department, Auburn University, Auburn, AL, USA (www.auburn.edu/)
Graphite nanosheets	Xiamen Knano Graphite Technology Co. Ltd (www.knano.com.cn/)

For startup companies, especially those investing in manufacturing nanoPCMs, cost-vs.-savings consideration is paramount. As discussed in the previous sections, the higher thermal conductivity of nanoPCMs may not be useful, and in some cases may be detrimental, from an energy-savings perspective. The thermophysical properties of the PCMs may need to be tailored for specific applications. As noted by Liu et al. (2015), the production efficiencies of nanoPCMs are not high enough to meet industrial demands, and it is a reasonable assumption that significant costs will be incurred in scaling up the production of nanoPCMs from laboratories to manufacturing plants. Therefore, manufacturing of PCMs, nano or otherwise,

needs to consider the end use, so practical energy savings and suitable returns on investments can be realized.

9.7. Summary and Conclusions

The nanoPCM-research till date has primarily focused on development of nano-enhanced PCMs and characterization of the thermo-physical properties or evaluation of melting rate, charging times, etc. In comparison, there are few studies that have evaluated the actual energy-related benefits of nano-enhanced PCMs in building applications.

From a material perspective, several successful approaches to creating nanoPCMs (both encapsulated PCM and PCM containing nano particles) have been investigated. The nanoPCMs that have been developed have usually shown enhanced thermal conductivity and some degradation of latent heat. Several studies have shown that the higher conductivity and lower latent heat resulted in increased melting rate and reduced charging time in thermal storage systems or heat exchangers. However, for 10% or lower concentrations of nanoparticles, the reductions in latent heat were within acceptable limits. The melting and freezing temperatures of nanoPCM were observed to be lowered with different concentrations of nanoparticles, but the reductions were not monotonous with increasing concentrations. The adding of nanoparticles also resulted in reductions in the subcooling of PCMs to various degrees based on concentration.

9.8. Future Research

While PCMs have been around for several decades, nanoPCMs are still in their infancy. However, there are several areas where further research is needed. Whole building simulations with PCMs are needed to estimate the potential for energy savings and for calculating the savings to cost ratio, but the current modelling tools are still works-in-progress. Well-validated numerical simulation tools for evaluation of nanoPCM applications are needed. Compared to macro-packaged PCMs, there are few empirical studies evaluating benefits of nanoPCM in actual building applications. Such studies are needed to both evaluate the in situ performance of nanoPCMs and to generate data that can be used for validating existing and new numerical simulation programs. Further, subcooling effects (i.e. different enthalpy functions for heating and cooling) are not captured by current simulation tools. The degree of subcooling itself is dependent both on the material and the rate of cooling of the PCM; the latter is a function of the application. Understanding and capturing the subcooling phenomenon is important for reliable estimates of PCM performance.

Another issue with PCMs is the limited long-term (10, 20, 30 years) data from building applications. Therefore, appropriate aging tests are needed to estimate the long term performance of PCMs. The aging tests being currently done are primarily based on temperature cycling only. It will be interesting to see if other environmental factors, moisture for example, have any impacts on the PCM packaging, chemical stability of the materials, etc., and cause any performance degradation.

Finally, cost vs. savings analyses of nanoPCMs are critical for startup companies so that they can make sound business-related decisions. The viability and economics of nanoPCMs are also related to issues like production efficiency, mass production and scale-up, development of cost-effective and low energy-intensity processes, scoping of newer materials that are well-suited to building applications, etc.

9.9. Nomenclature

B	Melt fraction
h	Enthalpy (J/g)
k	Thermal conductivity (W/m/K)
m, n	Number of water molecules
T	Temperature (K)

Subscripts:

l	Fully molten state of PCM
s	Fully frozen state of PCM

Abbreviations:

A/C	Air conditioning
CAV	Constant air volume
CNT	Carbon nanotube
DCV	Demand control ventilation
DSC	Differential scanning calorimetry
ECV	Economizer cycle ventilation
EDA	Ethylene diamine
EER	Energy efficiency ratio
HDPE	High density polyethylene
HFMA	Heat flow meter apparatus
MA	Myristic acid
MWCNT	Multi-walled carbon nanotube
NEPCM	Nanoencapsulated phase change material
NP	Nanoparticles
NTES	Nanoparticles embedded latent thermal energy storage system
PA	Palmitic acid

PCM	Phase change material
PS	Polystyrene
PVP	Poly Vinyl Pyrrolidone
SAT	Sodium acetate trihydrate
SEM	Scanning electron microscopy
SS	Sodium stearate
TEOS	Tetraethylorthosilicate
TDI	Tolylene diisocyanate
VAV	Variable air volume
xGnP	Exfoliated graphite nanoplatelets

9.10. Acknowledgement

This work was supported by the Building Technologies Office (BTO) of the U. S. Department of Energy under Contract No. DE-AC05-00OR22725 with UT-Battelle, LLC.

9.11. References

1. Abolghasemi M, Keshavarz A, Mehrabian MA. Heat transfer enhancement of a thermal storage unit consisting of a phase change material and nano-particles. J. Renewable Sustainable Energy 2012;4,043124.
2. Al-Saadi SN, Z Zhai. Modeling phase change materials embedded in building enclosure: A review. Renewable Sustainable Energy Reviews 2013;21:659-73.
3. Alshaer WG, Barrio EPD, Rady MA, Abdellatif OE, Nada SA. Analysis of the anomalous thermal properties of phase change materials based on paraffin wax and multi walls carbon nanotubes. Intl. J. Heat Mass Transfer – Theory and Applications (IREHEAT), 2013;1:297-307.
4. Ascione F, Bianco N, De Masi RF, de'Rossi F, Vanoli GP. Energy refurbishment of existing buildings through the use of phase change materials: Energy savings and indoor comfort in the cooling season. App. Energy 2014;113:990-1007.
5. ASTM C1784-13. 2013. Standard Test Method for Using a Heat Flow Meter Apparatus for Measuring Thermal Storage Properties of Phase Change Materials and Products. ASTM International, West Conshohocken, PA, USA.
6. ASTM C518-10. 2010. Standard Test Method for Steady-State Thermal Properties by Means of the Heat Flow Meter Apparatus. ASTM International, West Conshohocken, PA, USA.
7. Aydin AA, Okutan H. Polyurethane rigid foam composites incorporated with fatty acid ester-based phase change material. Energy Conv. Mgmt. 2013;68:74-81.

8. Biswas K, Abhari R. Low-cost phase change material as an energy storage medium in building envelopes: Experimental and numerical analyses. Energy Conv. Mgmt. 2014;88:1020-31.
9. Biswas K, Lu, J, Soroushian, P, Shrestha, S. Combined experimental and numerical evaluation of a prototype nano-PCM enhanced wallboard. App. Energy 2014;131:517-29.
10. Cabeza LF, Castellon C, Nogues M, Medrano M, Leppers R, Zubillaga O. Use of microencapsulated PCM in concrete walls for energy savings. Energy Build. 2007;39:113–9.
11. Castellon C, Gunther E, Mehling H, Hiebler S, Cabeza LF. Determination of the enthalpy of PCM as a function of temperature using a heat-flux DSC: A study of the different measurement procedures and their accuracy. Intl. J. Energy Res 2008;32:1258-65.
12. Chaabane M, Mhiri H, Bournot P. Thermal performance of an integrated collector storage solar water heater (ICSSWH) with phase change materials (PCM). Energy Conv. Mgmt. 2014;78:897-903.
13. Choi DH, Lee J, Hong H, Kang YT. Thermal conductivity and heat transfer performance enhancement of phase change materials (PCM) containing carbon additives for heat storage application. Intl J Refrigeration 2014;42:112-20.
14. Darkwa J, Su O. Thermal simulation of composite high conductivity laminated microencapsulated phase change material (MEPCM) board. App. Energy 2012;95:246-52.
15. Dhaidan NS, Khodadadi JM, Al-Hattab TA, Al-Mashat SM. Experimental and numerical investigation of melting of NePCM inside an annular container under a constant heat flux including the effect of eccentricity. Intl. J. Heat Mass Transfer 2013;67:455-68.
16. Fauzi H, Metselaar HSC, Mahlia TMI, Silakhori M. Thermo-physical stability of fatty acid eutectic mixtures subjected to accelerated aging for thermal energy storage (TES) application. App. Therm. Eng. 2014;66:328-34.
17. Gmelin E, Sarge SM. Temperature, heat and heat flow rate calibration of differential scanning calorimeters. Thermochimica Acta 2000;347:9-13.
18. Groulx D. Numerical study of nano-enhanced PCMs: Are they worth it? *Proc. First Thermal and Fluid Engineering Summer Conference*, August 2015, New York, USA.
19. Hawes DW, Feldman D. Absorption of phase change materials in concrete. Solar Energy Mater. Solar Cells 1992;27:91–101.

20. He Q, Wang S, Tong M, Liu Y. Experimental study on thermophysical properties of nanofluids as phase-change material (PCM) in low temperature cool storage. Energy Convers Manage 2012;64:199–205.
21. Ho CJ, Gao JY. Preparation and thermophysical properties of nanoparticle-in-paraffin emulsion as phase change material. Int Commun Heat Mass Transfer 2009;36:467–70.
22. Hong Y, Wub W, Huc J, Zhang M, Voevodin AA, Chow L, Su M. Controlling super-cooling of encapsulated phase change nanoparticles for enhanced heat transfer. Chem. Physics Letters 2011;504:180-4.
23. Hosseinizadeh SF, Darzi AAR, Tan FL. Numerical investigations of unconstrained melting of nano-enhanced phase change material (NEPCM) inside a spherical container. Intl. J. Thermal Sci. 2012;51:77-83.
24. Hu P, Lu D-J, Fan X-Y, Zhou X, Chen Z-S. Phase change performance of sodium acetate trihydrate with AlN nanoparticles and CMC. Sol Energy Mater Sol Cells 2011;95:2645–9.
25. Huang MJ, Eames PC, Norton B. Phase change materials for limiting temperature rise in building integrated photovoltaics. Solar Energy 2006;80:1121-30.
26. Jeong S, Chung O, Yu S, Kim S. Improvement of the thermal properties of Bio-based PCM using exfoliated graphite nanoplatelets. Solar Energy Mater. Solar Cells 2013;117:87–92.
27. Jeong S, Lee J, Seo J, Kim S. Thermal performance evaluation of Bio-based shape stabilized PCM with boron nitride for energy saving. Intl. J. Heat Mass Transfer 2014;71:245-50.
28. Latibari ST, Mehrali M, Mehrali M, Mahlia TMI, Metselaar HSC. Synthesis, characterization and thermal properties of nanoencapsulated phase change materials via sol-gel method. Energy 2013;61:664-72.
29. Karaipekli A, Sari A, Kaygusuz K. Thermal properties and thermal reliability of capric acid/stearic acid mixture for latent heat thermal energy storage. Energy Sources, Part A 2009;31(3):199-207.
30. Karunamurthy K, Kumar KMM, Suresh S. PCM based thermal energy storage system containing CuO nano-particles. Intl. J. Nanomaterials Tech 2012;3:13-16.
31. Khodadadi JM, Hosseinizadeh SF. Nanoparticle-enhanced phase change materials (NEPCM) with great potential for improved thermal energy storage. Intl. Comm. Heat Mass Transfer 2007;34:534-43.
32. Kibria MA, Anisur MR, Mahfuz MH, Saidur R, Metselaar IHSC. A review on thermophysical properties of nanoparticle dispersed phase change materials. Energy

Conv. Mgmt. 2015; 95:69-89.

33. Kosny J, Kossecka E, Brzezinski A, Tleoubaev A, Yarbrough D (2012a). Dynamic thermal performance analysis of fiber insulations containing bio-based phase change materials (PCMs). Energy Build. 2012;52:122-31.
34. Kosny J, Biswas K, Miller W, Kriner S (2012b). Field thermal performance of naturally ventilated solar roof with PCM heat sink. Solar Energy 2012;86:2504-14.
35. Liu C, Rao Z, Zhao J, Huo Y, Li Y. Review on nanoencapsulated phase change materials: Preparation, characterization and heat transfer enhancement. Nano Energy 2015;13:814-26.
36. Lu W, Tassou SA. Experimental study of the thermal characteristics of phase change slurries for active cooling. App. Energy 2012;91:366-74.
37. Meng E, Yu H, Zhan G, He Y. Experimental and numerical study of the thermal performance of a new type of phase change material room. Energy Conv. Mgmt. 2013;74:386-94.
38. Meng X, Zhang H, Sun L, Xu F, Jiao Q, Zhao Z, et al. Preparation and thermal properties of fatty acids/CNTs composite as shape-stabilized phase change materials. J Therm Anal Calorim 2012:1–8.
39. Parameshwaran R, Jayavel R, Kalaiselvam S. (2013a) Study on thermal properties of organic ester phase-change material embedded with silver nanoparticles. J. Therm. Anal. Calorim. 2013; 114:845-58.
40. Parameshwaran R, Dhamodharan P, Kalaiselvam S. (2013b) Study on thermal storage properties of hybrid nanocomposite-dibasic ester as phase change material. Thermochim. Acta 2013;573:106–20.
41. Parameshwaran R, Kalaiselvam S. Energy conservative air conditioning system using silver nano-based PCM thermal storage for modern buildings. Energy Build. 2014; 69:202-12.
42. Parameshwaran R, Kalaiselvam S. Nanomaterial-embedded phase-change materials (PCMs) for reducing building cooling needs, in: *Eco-Efficient Materials for Mitigating Building Cooling Needs*, edited by F Pacheco-Torgal et al. (Woodhead, Cambridge, 2015), pp 401–439.
43. Park S, Lee Y, Kim YS, Lee HM, Kim JH, Cheong IW, Koh W-G. Magnetic nanoparticle-embedded PCM nanocapsules based onparaffin core and polyurea shell. Colloids Surfaces A: Physicochemical Eng. Aspects 2014;450:46-51.
44. RAL-GZ 896. Phase Change Material, Quality Assurance. German Institute for Quality Assurance and Certification E.V. September 2009.

45. Sánchez-Silva L, Tsavalas J, Sundberg D, Sánchez P, Rodriguez JF. Synthesis and characterization of paraffin wax microcapsules with acrylic-based polymer shells. Ind. Eng. Chem. Res 2010;49:12204–11.
46. Sari A. Thermal reliability test of some fatty acids as PCMs used for solar thermal latent heat storage applications. Energy Conv. Mgmt. 2003;44(14):2277-87.
47. Sari A, Alkan C, Döğüşcü DK, Biçer A. Micro/nano-encapsulated n-heptadecane with polystyrene shell for latent heat thermal energy storage. Solar Energy Mater. Solar Cells 2014;126:42-50.
48. Sayyar M, Weerasiri RR, Soroushian P, Lu J. Experimental and numerical study of shape-stable phase-changenanocomposite toward energy-efficient building constructions. Energy Build. 2014;75:249-55.
49. Sharma SD, Buddhi D, Sawhney RL. Accelerated thermal cycle test of latent heat-storage materials. Solar Energy 1999;66(6):483-90.
50. Sharma A, Tyagi VV, Chen CR, Buddhi D. Review on thermal energy storage with phase change materials and applications. Renewable Sustainable Energy Reviews 2009;13:318-45.
51. Shi X, Memon SA, Tang W, Cui H, Xing F. Experimental assessment of position of macro encapsulated phase change material in concrete walls on indoor temperatures and humidity levels. Energy Build. 2014;71:80-7.
52. Shrestha S, Miller W, Stovall T, Desjarlais A, Childs K, Porter W, et al. Modeling PCM-enhanced insulation system and benchmarking EnergyPlus against controlled field data. *Proc. Building Simulation 2011: 12th Conf. International Building Performance Simulation Association*, p 800-7, 2011, available online at http://www.ibpsa.org/proceedings/BS2011/P_1328.pdf.
53. Wang X, Zhang L, Yu Y-H, Jia L, Mannan MS, Chen Y, Cheng Z. Nano-encapsulated PCM via Pickering Emulsification. Scientific Reports 2015; 5, DOI: 10.1038/srep13357, http://www.nature.com/articles/srep13357.
54. Wu W-F, Liu N, Cheng W-L, Liu Y. Study on the effect of shape-stabilized phase change materials on spacecraft thermal control in extreme thermal environment. Energy Conv. Mgmt. 2013;69:174-80.
55. Yanshan L, Shujun W, Hongyan L, Fanbin M, Huanqing M, Wangang Z. Preparation and characterization of melamine/formaldehyde/ polyethylene glycol crosslinking copolymers as solid–solid phase change materials. Solar Energy Mater. Solar Cells 2014;127:92-7.
56. Yavari F, Fard HR, Pashayi K, Rafiee MA, Zamiri A, Yu Z, et al. Enhanced thermal

conductivity in a nanostructured phase change composite due to low concentration graphene additives. J Phys Chem C 2011;115:8753–8.

57. Zalba B, Marin JM, Cabeza LF, Mehling H. Review on thermal energy storage with phase change: materials, heat transfer analysis and applications. App. Therm. Eng. 2009;23:251-83.
58. Zeng J, Cao Z, Yang D, Xu F, Sun L, Zhang X, et al. Effects of MWNTs on phase change enthalpy and thermal conductivity of a solid-liquid organic PCM. J Therm Anal Calorim 2009;95:507–12.
59. Zeng J, Cao Z, Yang D, Sun L, Zhang L. Thermal conductivity enhancement of Ag nanowires on an organic phase change material. J Therm Anal Calorim 2010;101:385–9.
60. Zhang X, Niu J, Wu J-Y, Zhang S. The application of modified multi-wall carbon nano-tube particles in PCM as the nucleating agent. App. Mechanics Mater. 2013;328:753-57.
61. Zhou D, Zhao CY, Tian, Y. Review on thermal energy storage with phase change materials (PCMs) in building applications. App. Energy 2012;92:593-605.
62. Zhou G, Zhang Y, Wang X, Lin K, Xiao W. An assessment of mixed type PCM-gypsum and shape-stabilized PCM plates in a building for passive solar heating. Solar Energy 2007;81: 1351-60.
63. Zwanzig SD, Lian Y, Brehob EG. Numerical simulation of phase change material composite wallboard in a multi-layered building envelope. Energy Conv. Mgmt. 2013;69:27-40.